This is the accepted manuscript made available via CHORUS. The article has been published as:

Matrix element method and QCD radiation

J. Alwall, A. Freitas, and O. Mattelaer

Phys. Rev. D **83**, 074010 — Published 12 April 2011

DOI: 10.1103/PhysRevD.83.074010

DZ10769

CP3–10–35

The Matrix Element Method and QCD Radiation

J. Alwall[1], A. Freitas[2], O. Mattelaer[3]

[1] *Department of Physics and National Center for Theoretical Sciences, National Taiwan University, Taipei, 10617, Taiwan*

[2] *Department of Physics & Astronomy, University of Pittsburgh, 3941 O'Hara St, Pittsburgh, PA 15260, USA*

[3] *Center for Cosmology, Particle Physics and Phenomenology (CP3), Université Catholique de Louvain, Chemin du Cyclotron 2, 1348 Louvain-la-Neuve, Belgium*

REVIEW COPY
NOT FOR DISTRIBUTION

Abstract

The matrix element method (MEM) has been extensively used for the analysis of top-quark and W-boson physics at the Tevatron, but in general without dedicated treatment of initial state QCD radiation. At the LHC, the increased center of mass energy leads to a significant increase in the amount of QCD radiation, which makes it mandatory to carefully account for its effects. We here present several methods for inclusion of QCD radiation effects in the MEM, and apply them to mass determination in the presence of multiple invisible particles in the final state. We demonstrate significantly improved results compared to the standard treatment.

1 Introduction

The discovery and analysis of new physics particles, beyond the Standard Model, is one of the main goals for building the Large Hadron Collider (LHC). The presence of such new physics at an energy scale accessible by the LHC is indicated by shortcomings of the Standard Model, in particular its inability to explain the stability of the Higgs boson mass and the nature of the cosmological dark matter. New physics models which simultaneously explain these two riddles have certain common features: strongly produced particles charged under QCD, which are perhaps exclusively pair-produced and decay (mainly or exclusively) to stable invisible particles (*i. e.*, particles with negligible interactions with the detector material). Even if the new physics includes singly produced resonances, these might very well decay mainly to final states including invisible particles.

The analysis of new physics processes with invisible particles in the final state is particularly challenging, due to the absence of invariant mass peaks. Even the determination of masses of the new particles typically requires large statistics [1]. This difficulty is further enhanced by the presence of QCD radiation (in particular initial-state radiation, *i. e.* QCD radiation that is not collinear with any of the decay products), which complicates the final states in several ways: by adding additional jets (that do not correspond to any decay products of the produced new physics particles), and by modifying the kinematics of the decay products through emission of particles with sizeable transverse momenta, which result in transverse boosts of the decay products.

Among the methods for extraction of model parameters, the one which takes into account the most information from the experimental events is the Matrix Element Method (MEM) [2]. The MEM has been used extensively for top quark physics by the experimental collaborations at the Tevatron [3], and has resulted in the most precise measurement of the top quark mass to date. The method is described in detail in section 2, and it here suffices to say that it uses the theoretical squared matrix element for the process to give a weight for each experimental event, for a given point in the parameter space of the model. One drawback of the method in its basic form is that only events with final states that perfectly match those in the considered matrix element can be used. While this is not a big problem at the Tevatron, where the phase space for additional QCD radiation is limited by the relatively low center-of-mass energy, events at the LHC have a large phase space for QCD radiation. It is therefore of crucial importance to develop the MEM to account also for such additional radiation.

In this paper, we suggest several methods to account for additional QCD radiation in processes with invisible particles in the final state, either by explicitly correcting for the QCD emission or by parametrizing its effect through an appropriate function. Partial results have already been reported in Ref. [4], but this paper provides a more extensive and detailed analysis. It is organized as follows: In section 2, we describe the details of the MEM. Section 3 is dedicated to the study of the MEM with initial-state QCD radiation at the parton level, using the parton shower Monte Carlo generator Pythia [5]. We study two example processes, top quark pair production with di-leptonic decay giving neutrinos as decay products for both top quarks, and Standard Model Higgs boson production with

decay to $W^+W^- \to l^+l^-\nu\bar{\nu}$. Although these are both Standard Model processes, they are representative for the type of new physics we are targeting—heavy particles with invisible particles in their decays, which makes it impossible to reconstruct the complete final state of any of the produced particles. In section 4, we turn to the more complicated case where both QCD radiation and hadronization as well as detector effects are taken into account. We give our conclusions in section 5.

Note that similar approaches to include QCD radiation have been explored by the D0 and CDF collaborations in Refs. [6].

2 The Matrix Element Likelihood Method

The Matrix Element Method (MEM) [2] provides a recipe for computing a likelihood that an experimental event agrees with a theoretical model. The information about the theoretical model is supplied in the form of the squared matrix element for a concrete process. One or several parameters of the model can be determined from the data by finding the maximum of the likelihood for a sample of events as a function of the parameters.

The likelihood measure for a single event, with measured momenta $\mathbf{p}_i^{\text{vis}}$, to agree with the model, given a set of parameters α, is defined as

$$\mathcal{P}(\mathbf{p}_i^{\text{vis}}|\alpha) = \frac{1}{\sigma_\alpha}\int dx_1 dx_2 \frac{f_1(x_1)f_2(x_2)}{2sx_1x_2}\left[\prod_{i\in\text{final}}\int\frac{d^3p_i}{(2\pi)^3 2E_i}\right]|M_\alpha(p_i)|^2\prod_{i\in\text{vis}}\delta(\mathbf{p}_i-\mathbf{p}_i^{\text{vis}}). \quad (1)$$

Here f_1 and f_2 are the parton distribution functions, M_α is the theoretical matrix element, and σ_α is the total cross section, computed with the same matrix element. The normalization ensures that

$$\left[\prod_{i\in\text{vis}}\int d^3p_i^{\text{vis}}\right]\mathcal{P}(\mathbf{p}_i^{\text{vis}}|\alpha) = 1. \quad (2)$$

The three-momenta $\mathbf{p}_i^{\text{vis}}$ of the visible measured objects are matched with the corresponding momenta $\mathbf{p}_i$ of the final state particles in the matrix elements, while the momenta of invisible particles (neutrinos or weakly interacting new physics particles) are integrated over.

Quarks and gluons are matched with jets as visible objects, whose energy is typically not measured very precisely. Therefore one has to include a transfer function W for jets, which parametrizes the combined effects of parton showering, hadronization and detector response:

$$\mathcal{P}(\mathbf{p}_i^{\text{vis}}|\alpha) = \frac{1}{\sigma_\alpha}\int dx_1 dx_2 \frac{f_1(x_1)f_2(x_2)}{2sx_1x_2}\left[\prod_{i\in\text{final}}\int\frac{d^3p_i}{(2\pi)^3 2E_i}\right]|M_\alpha(p_i)|^2\prod_{i\in\text{vis}}W_i(\mathbf{p}_i,\mathbf{p}_i^{\text{vis}}). \quad (3)$$

For leptons and photons it is mostly sufficient to approximate the transfer functions by a delta function, as above.

For a sample of N events, the combined likelihood is usually stated in terms of its logarithm:

$$-\ln(\mathcal{L}) = -\sum_{n=1}^{N} \ln \mathcal{P}(\mathbf{p}_{n,i}^{\mathrm{vis}}|\alpha) + N \left[\prod_{i \in \mathrm{vis}} \int d^3 p_i^{\mathrm{vis}} \right] \mathrm{Acc}(\mathbf{p}_i^{\mathrm{vis}})\, \mathcal{P}(\mathbf{p}_i^{\mathrm{vis}}|\alpha), \tag{4}$$

where $\mathbf{p}_{n,i}^{\mathrm{vis}}$ are the measured momenta of the nth event.* The acceptance function $\mathrm{Acc}(\mathbf{p}_i^{\mathrm{vis}})$ corrects for the bias introduced by detector acceptance and event selection†.

The MEM has been used extensively for top quark physics by the experimental collaborations at the Tevatron [3]. At this time, the most precise determination of the top quark mass has been achieved with this technique, which can be attributed to the fact that in principle it takes into account all relevant experimental information. In most Tevatron analyses‡, only events for which the number of jets exactly matches the number of colored partons in the hard matrix element have been included. For instance, only two-jet events have been considered for the analysis of the di-leptonic top-quark pairs. At the Tevatron this approach works, since the top quarks are relatively heavy compared to the beam energy and thus the phase space for extra radiation is highly suppressed.

However, at the LHC radiation of hard jets is expected to be abundant, not only for top pair production but also for new physics processes involving colored particles with masses of a few 100 GeV [7]. With a center-of-mass energy of 14 TeV, the number of top pair events is reduced by more than 40% if a cut on extra jets with $p_{\mathrm{T}} > 40$ GeV is imposed§. This estimate is based on events generated with Pythia 6.4 [5] and passed through the fast detector simulation Pgs 4 [8]. As will be shown later, even the presence of additional jets with $p_{\mathrm{T}} < 40$ GeV can lead to problems with fitting the signal events, so that a tighter cut will be necessary to sufficiently reduce the influence of jet radiation, hence leading to a large loss of signal statistics.

Alternatively, one could try to take into account events with extra jets by including matrix elements with more partons in the final state. Referring again to the example of di-leptonic top quark pairs, this would amount to matrix elements corresponding to the processes $pp \to b\bar{b}l^+l^-\nu\bar{\nu} + n_q q + n_{\bar{q}}\bar{q} + n_g g$, which have n_q quarks, $n_{\bar{q}}$ antiquarks and n_g gluons in the final state besides the usual top decay products. While this approach should allow to correctly include all events, it substantially increases the computation time, due to the complexity of the multi-particle matrix elements, the more complicated structure of the

*In the likelihood, we have neglected the term $\sum_{n=1}^{N} \ln(\mathrm{Acc}(\mathbf{p}_{n,i}^{\mathrm{vis}}))$ since it is independent of any theoretical parameters α.

†When using selection cuts pertaining to individual jets, the likelihood can be shifted by a small bias even when the acceptance function is properly incorporated in the calculation. This is related to the fact that the transfer functions W_i only imperfectly model the effect of extra jets from final-state radiation. For the content of this paper this bias is irrelevant, since we mainly focus on the role of initial-state radiation, but let us remark that in principle one could construct an un-biased estimator with a more sophisticated parametrization of the transfer functions.

‡See Ref. [6] for approaches including extra jets.

§About 27% of events have one additional jet with $p_{\mathrm{T}} > 40$ GeV, while about 15% have two or more extra jets.

phase space, and the combinatorics related to summing over quark flavors and gluons in the extra jets. Even if one restricts oneself to considering only up to one extra parton in the final state, the computing intensity of the likelihood fit is increased by more than one order of magnitude.

The large majority of extra jets originates from initial-state radiation (ISR). In the following two sections, several methods will be described which account for the main effect of ISR by performing kinematical corrections event by event, using matrix elements for the hard process only, without additional partons in the final state.

For concreteness, the numerical analyses in the following sections has been carried out for two representative processes with invisible particles in the decay, so that the final state is not fully reconstructable. Top-quark pair production with di-leptonic decay,

$$pp \to t\bar{t} \to b\bar{b}l^+l'^-\nu_l\bar{\nu}_{l'}, \tag{5}$$

is a typical case of pair production of heavy particles with relatively long and not fully reconstructable decay chains. As a second example we will consider Higgs production via gluon fusion,

$$pp \to gg \to h \to W^+W^- \to l^+l'^-\nu_l\bar{\nu}_{l'}, \tag{6}$$

with the characteristic features of a s-channel resonance.

Numerical results shown in the following sections correspond to a center-of-mass energy of $\sqrt{s} = 14$ TeV, but the essential aspects do not change for lower values of $\sqrt{s}$. Two independent implementations of the MEM are employed: the first is a specialized private code written by us using matrix elements generated by CompHEP 4.4 [9], the second is the flexible automated public tool MadWeight [10], which is based on the MadGraph/MadEvent framework [11].

The core task of both programs is the evaluation of the integration in eqs. (1), (3). For the process (5) this involves eight integration variables (six momentum components for the neutrino and the anti-neutrino, plus x_1 and x_2), but energy-momentum conservation reduces it to a four-dimensional integration. Instead of the final state (anti-)neutrino momenta, we use the invariant masses of the top quarks and W bosons as integration variables, since the integrand has sharp resonance peaks as function of these variables. The transformation between the neutrino momenta and the intermediate invariant masses involves the solution of a coupled system of two quadratic equations, which can be performed analytically. The final expressions are rather long and will therefore not be shown here (see Ref. [10] for examples). The Breit-Wigner resonances of the form

$$\frac{1}{(q_k^2 - m_k^2)^2 + m_k^2\Gamma_k^2}, \qquad (k = t, \bar{t}, W^+, W^-), \tag{7}$$

in the integrand can be mapped out by the additional variable transformation

$$q_k^2 = m_k^2 + m_k\Gamma_k \tan t_k, \qquad \frac{d(q_k^2)}{dt_k} = \frac{(q_k^2 - m_k^2)^2 + m_k^2\Gamma_k^2}{\pi m_k\Gamma_k}, \tag{8}$$

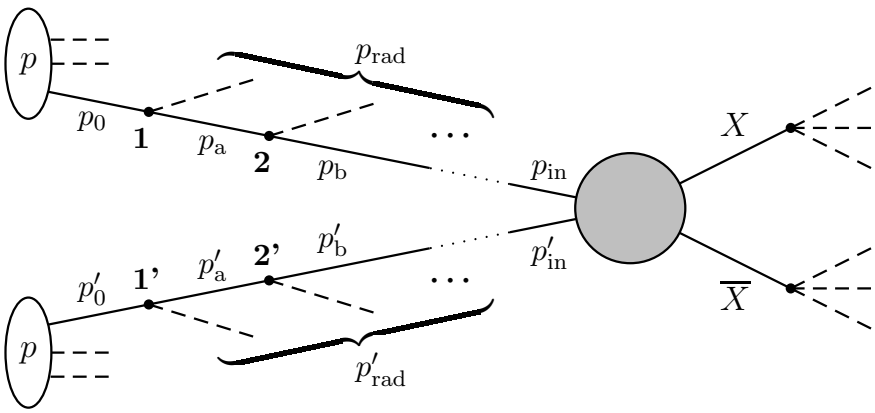

Figure 1: Schematic depiction of the event topology for pair production of heavy particles X, together with initial state radiation.

so that as a function of the t_k the integrand becomes almost flat across the entire region $-\pi/2 \leq t_k \leq \pi/2$ and the integration can be performed numerically without difficulty. The outputs of the two programs agree very well for all results shown in the following sections.

3 Initial State Radiation at Parton Level

In this section we restrict ourselves to an analysis at the parton level. Simulated "data" events have been generated with Pythia 6.4 [5] using CTEQ6L1 parton distribution functions [12]. The momenta of the final state particles in (5) or (6), as well as those of the initial state radiation, have been extracted from the Pythia event record for each event. No cuts on the parton momenta have been implemented and therefore the acceptance term in (4) is simply 1. This allows us to single out the effects of ISR without complications from final state radiation, hadronization, underlying event and detector efficiencies. For simplicity and clarity of the discussion, we do not include backgrounds in the analysis.

The first technique that we propose here is based on the observation that the most significant effect of ISR is on the kinematics of the events; without proper inclusion of ISR the momentum balance of the decay products is violated. The proper kinematics of the hard scattering matrix element can be restored by simply boosting the hard event by the momenta of the ISR. Since the longitudinal incoming momenta are integrated over in the computation of the likelihood, see eqs. (1) and (3), it is sufficient to perform the boost for the transverse coordinates only. In practice, instead of boosting the measured final state momenta, we perform the boost on the incoming partons of the matrix element, which is equivalent since the squared matrix element is a Lorentz scalar. With this technique we are only performing a kinematical boost, which allows us to sum up the ISR momenta for each incoming leg—the sequence of individual branchings does not play any rôle.

This boost correction is the simplest possible treatment of ISR, which only maintains the proper momentum balance, while the effects of the particular QCD vertices and internal propagators (labeled by numbers and $p_{a,b,\ldots}$ in Fig. 1, respectively) are not taken into account.

It has the advantage of not increasing the computing time of the MEM likelihood fit compared to the situation without ISR.

However, one can try to do better by including Sudakov reweighting for the ISR. The Sudakov factor corresponds to the probability for no branching to occur between two scales $p^2_{\mathrm{T},E1} < p^2_{\mathrm{T},E0}$. For ISR it is appropriate to formulate the Sudakov factor in terms of backwards evolution from the hard process to the incident proton. In this case it is given by

$$\Delta_{\mathrm{ISR}}(p^2_{\mathrm{T},E0}, p^2_{\mathrm{T},E1}) = \exp\left(- \int_{p^2_{\mathrm{T},E1}}^{p^2_{\mathrm{T},E0}} \frac{d(p^2_{\mathrm{T},E})}{p^2_{\mathrm{T},E}} \frac{\alpha_{\mathrm{s}}(p^2_{\mathrm{T},E})}{2\pi} \sum_{j\in\{j\to i+X\}} \int_{z_{\min}(p^2_{\mathrm{T},E})}^{z_{\max}(p^2_{\mathrm{T},E})} dz \frac{P_{j\to i}(z)}{z} \frac{f_j(x_i/z, p^2_{\mathrm{T},E})}{f_i(x_i, p^2_{\mathrm{T},E})} \right) \quad (9)$$

where the sum runs over all possible assignments of partons i, j (quarks or gluon) in the branching $j \to i + X$. Here $P_{j\to i}$ are the splitting functions, which for massless quarks read

$$P_{qq}(z) = P_{qg} = \frac{4(1+z^2)}{3(1-z)}, \quad P_{gq}(z) = \frac{1}{2}\left[z^2 + (1-z)^2\right], \quad P_{gg}(z) = 6\frac{[1-z(1-z)]^2}{z(1-z)}. \quad (10)$$

Furthermore, z is the ratio between the pre-branching invariant mass squared of the parton-parton interaction and the post-branching invariant mass squared.

To account for the proper weight of the ISR, one needs the probability of having a splitting $j \to i + X$ at some kinematic configuration $(p^2_{\mathrm{T},E}, z)$, which is given by taking the derivative of the Sudakov factor:

$$\mathcal{P}_j(p^2_{\mathrm{T},E}, z) = -\frac{d^2}{d(p^2_{\mathrm{T},E})dz} \Delta_{\mathrm{ISR}}(p^2_{\mathrm{T},E0}, p^2_{\mathrm{T},E}) \quad (11)$$

$$= \frac{\alpha_{\mathrm{s}}(p^2_{\mathrm{T},E})}{2\pi p^2_{\mathrm{T},E}} \frac{P_{j\to i}(z)}{z} \frac{f_j(x_i/z, p^2_{\mathrm{T},E})}{f_i(x_i, p^2_{\mathrm{T},E})} \Delta_{\mathrm{ISR}}(p^2_{\mathrm{T},E0}, p^2_{\mathrm{T},E}) \quad (12)$$

The branching probability for any kind of parton is then given by $\sum_j \mathcal{P}_j(p^2_{\mathrm{T},E}, z)$.

Evidently it is not possible to reconstruct the entire sequence of ISR branchings in the correct order from the event data. For most events, however, one microscopic branching process carries most p_{T} of all ISR from one leg, so that a reasonable approximation can be obtained by adding up all ISR momenta stemming from one leg and calculating the Sudakov factor for one single branching with the summed momentum $p^2_{\mathrm{T},E} = p^2_{\mathrm{T,ISR}}$.

Since the ISR tends to be emitted at low angles, we approximate the ratio z by the longitudinal momentum components,

$$z \approx \frac{p_{\mathrm{in,z}}}{p_{\mathrm{in,z}} + p_{\mathrm{rad,z}}}, \quad (13)$$

where p_{in} is the momentum of the incoming parton of the hard collision process and p_{rad} is the momentum of the ISR associated with this leg, see Fig. 1.

Fig. 2 shows numerical results for the MEM likelihood fit for the example of top-quark pair production with di-leptonic decays, eq. (5). For reference, the solid curve shows the idealized

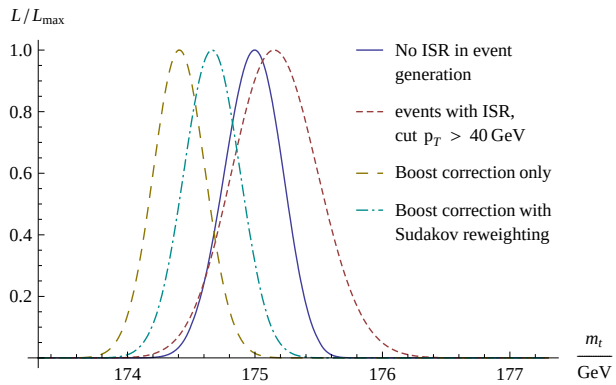

Figure 2: Reconstruction of the top quark mass from a matrix element likelihood fit to 1000 parton-level di-lepton $t\bar{t}$ events at the LHC with $\sqrt{s} = 14$ TeV. A top mass of $m_t = 175$ GeV has been used for the event generation. Shown in the plot are the idealized situation without ISR in the event generation (solid curve), the influence of ISR if no correction method is used (short dashed), the result for application of the kinematic boost correction only (long dashed), and the boost correction with Sudakov reweighting (dash-dotted). The likelihood reflects statistical errors only.

situation without ISR in the event generation, so that the events are directly produced by the same matrix element that is used in the matrix element analysis, and contain exactly two b-quarks and two leptons. The short-dashed curve corresponds to event generation with ISR, but ISR is not accounted for in the likelihood fit; instead events with ISR with combined $p_{\mathrm{T}} > 40$ GeV have been vetoed. In this (parton-level) case, the fit yields a central value for the top quark mass close to the true input value, but the statistical uncertainty is increased by a factor of about 1.5 (as can be seen from the larger width of the curve).

The other curves in Fig. 2 demonstrate the effect of the boost correction. As expected, the statistical error is not increased by this method. Applying only the kinematical boost correction, without the Sudakov reweighting, leads to a central value for the fitted top mass that is shifted downwards by about 0.5 GeV. While this is still marginally consistent within errors, it is indicative of a slight bias. If in addition the Sudakov factor (12) is included, the central value of the reconstructed top mass is much closer to the true input value and fully consistent within errors.

Fig. 3 shows results for Higgs production with decay to $l^+l'^-\nu_l\bar{\nu}_{l'}$ through a pair of W bosons, see (6). As we can see from the figure, such s-channel resonance processes are even more sensitive to the influence of ISR. Indeed, the Higgs mass is not properly reconstructed by the MEM likelihood fit even if ISR jets with $p_{\mathrm{T}} > 40$ GeV are vetoed—it is only when the veto threshold is lowered to an unrealistically low value of 6 GeV that the fit becomes marginally consistent with the correct input value $m_h = 180$ GeV. On the other hand, the purely kinematical boost correction (without reweighting) already yields a fit result that is very close to $m_h = 180$ GeV, while inclusion of the Sudakov reweighting leads to near-perfect agreement with the input value.

This strong sensitivity of the MEM fit to ISR is a particular feature of processes with

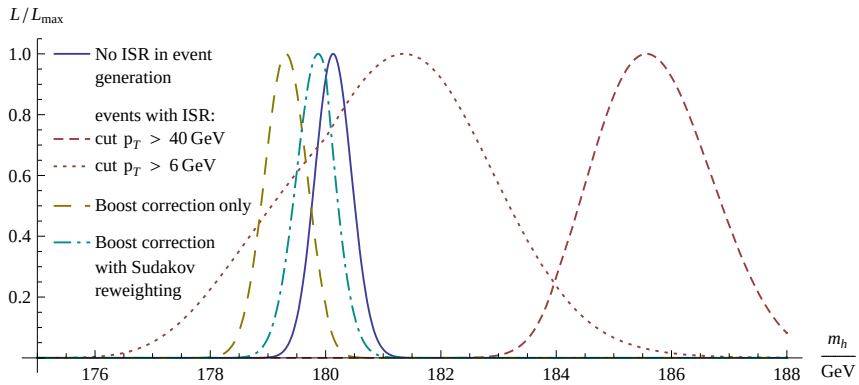

Figure 3: Reconstruction of the Higgs boson mass from a matrix element likelihood fit to 1000 parton-level di-lepton events at the LHC with $\sqrt{s} = 14$ TeV. A Higgs mass of $m_h = 180$ GeV has been used for the event generation, so that the W^+W^- channel is open and dominant. The plot compares the idealized situation without ISR in the event generation (solid curve) with simulation results including ISR, and either no correction (short dashed and dotted), purely kinematical boost correction (long dashed), or boost correction with Sudakov reweighting (dash-dotted). The likelihood reflects statistical errors only.

narrow s-channel resonances, where $\Gamma_{\rm res} \ll m_{\rm res}$ [*e. g.* process (6) with $m_h = 180$ GeV and $\Gamma_h \approx 0.6$ GeV]. When ignoring ISR with transverse momenta of a few GeV, it can become impossible to find final-state momentum configurations where both the W boson and the Higgs propagators are on-shell for a given event, since the magnitude of the momentum mismeasurement is larger than the Higgs width. Many events will therefore be poorly or wrongly reconstructed. In contrast, a pair production process without an s-channel resonance is much less sensitive to the precise value of the incident momenta $p_{\rm in}^{(\prime)}$.

While the application of the boost correction method is straightforward at the parton level, the situation becomes more complex in a more realistic framework with jet fragmentation and hadronization, as will be shown in the next section.

4 Initial State Radiation at Hadron Level

In this section the influence of ISR is investigated in a setup including parton showering, hadronization and a simple detector simulation in the event generation. As before, events have been generated with Pythia 6.4 [5], but now using fully hadronized events and including underlying event from additional parton interactions. These events have been passed through the fast detector simulation Pgs 4 [8] with general LHC detector parameters. For top-quark pair production with di-leptonic decay (eq. (5)), all events in the sample are required to contain two reconstructed leptons and at least two reconstructed jets with $p_{\rm T} > 50$ GeV, but no other selection cuts have been applied besides the intrinsic detector acceptance. The acceptance function in eq. (4) has been determined by producing one million events with Pythia/Pgs for each m_t value in the fit, and counting the number of events that

pass the selection cut. To account for jet smearing, a double-Gaussian transfer function (see eq. (3)) has been included for the jet energies, where the parameters of the double-Gaussian function have been tuned to a large sample of $t\bar{t}$ Monte-Carlo events generated with PYTHIA and passed through PGS.[¶] For the lepton energies and all angular variables, simple delta functions have been used in lieu of transfer functions.

For events with more than two jets, we assume that the extra jets come from ISR. In principle, heavy flavor tagging could be used to discriminate between the b jets from top decay and the ISR, which is comprised mostly of light-quark jets. Since the b jet identification is not unique, one would need to take into account the appropriate b-tagging efficiencies. However, this possibility is highly process-specific and would not work for processes where the heavy particles decay into light jets only, and we therefore choose not to exploit it here. For the sake of generality, we take the most conservative approach, and consider all permutations of the jets in the event, irrespective of their flavor content, as candidates to come from the top quark decay[‖]. The remaining jets are interpreted as stemming from ISR, where all jets reconstructed by PGS are included, without applying any additional cuts. The likelihoods for the permutations are added to form the event likelihood. Although most of these permutations correspond to incorrect jet-parton assignments, the amount of noise introduced into the fit is negligible since the wrong jet assignments typically result in very small likelihood values.

Fig. 4 shows how ISR can affect the likelihood fit in this more realistic case, if it is not accounted for in the matrix element treatment. The solid curve again shows the situation without ISR in the event generation[**]. The short-dashed curve corresponds to inclusion of ISR in the event generation but not in the MEM likelihood fit, and events with more than two jets with $p_{\mathrm{T}} > 40$ GeV have been excluded from the fit. In spite of this cut, the central value for the fitted top mass is shifted significantly compared to the input value $m_t = 175$ GeV, a feature that was not observed in the parton-level analysis (see Fig. 2). It can be explained by the fact that ISR typically generates multiple jets per events, and even if each jet has $p_{\mathrm{T}} < 40$ GeV, the total transverse ISR momentum can be considerably larger. In events with very hard ISR, the kinematics of the final state particles are substantially modified, so that the phase-space integration for matrix elements without ISR correction is sometimes pushed into an unphysical region. In such a situation, the fit results can depend on the details of the computer implementation of the MEM, and do not yield any meaningful information.

The situation improves somewhat when the jet p_{T} cut is lowered to 20 GeV (dotted curve in Fig. 4), but the fit result is still clearly inconsistent with the input value $m_t = 175$ GeV. Moreover, such a low p_{T} cut will be subject to large systematic experimental uncertainties.

It is therefore necessary to take into account and correct for ISR in the MEM fit. In order to perform the boost correction described in Section 3, each ISR jet needs to be associated

[¶]ISR has been turned off for the generation of these events, since it otherwise would affect the fit.

[‖]If an event has more than four jets we only permute the four hardest jets to save computing time.

[**]Even in the case without any ISR, the likelihood can be subject to a small bias caused by final-state radiation. This bias can in principle be eliminated by correcting the transfer functions for the effect of final-state radiation; see also footnote † on page 2.

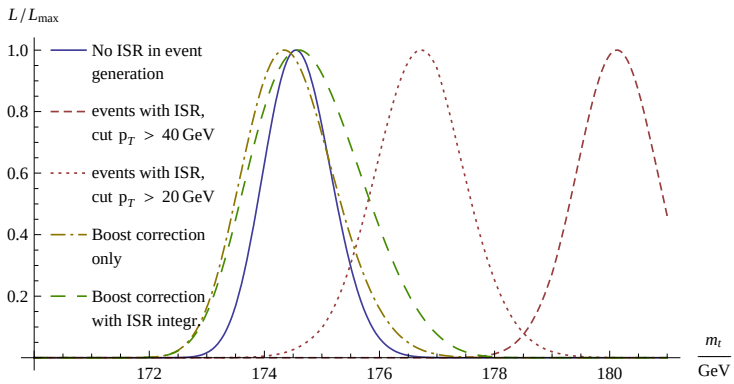

Figure 4: Reconstruction of the top quark mass from a matrix element likelihood fit to 1000 hadron-level di-lepton $t\bar{t}$ events at the LHC with $\sqrt{s} = 14$ TeV. A top mass of $m_t = 175$ GeV has been used for the event generation. The solid curve corresponds to the idealized situation without ISR in the event generation, while the result for uncorrected ISR is shown for a veto on extra jets with $p_{\mathrm{T}} > 40$ GeV (short dashed) and $p_{\mathrm{T}} > 20$ GeV (dotted). Also shown are the effect of the purely kinematical boost correction (dash-dotted) and the boost correction with ISR transfer functions (long dashed). The likelihood reflects statistical errors only.

with one of the incoming legs. A simple rule is to assume that jets in the left hemisphere stem from the incident parton coming from the right, and *vice versa*. As a first step, we will not include resolution functions for the ISR (in contrast to the other jets), in order to minimize the computing time, but we will comment on their rôle later. Similar to the parton-level analysis, the application of the kinematical boost correction (dash-dotted curve) leads to a considerably better agreement with the input value for the top mass.

As evident from the figure, the purely kinematical boost correction already leads to a satisfactory likelihood fit for top-quark pair production events. The situation is different, however, for processes with a narrow s-channel resonance, like Higgs production (6). We have seen already at parton level that this class of processes is very sensitive to ISR. Numerical results for the MEM fit are shown in Fig. 5, which shows that the boost correction does not lead to a good fit. This can be explained by the fact that on average the measured ISR jet momenta do not agree sufficiently well with the parton-level ISR momenta. Such measurement inaccuracies have a substantial impact for Higgs production process due to its strong sensitivity on the p_{T} of ISR.

While inclusion of Sudakov corrections was successful in the pure parton level case of Section 3, it turns out to be less useful in the fully hadronic case, and hardly improves the results from the pure boost correction. The reason for this is that the imperfect reconstruction of ISR in the detector has a much bigger impact on the likelihood fit.

There is however another way to account for these strong ISR effects, which drastically reduces the dependence on the detector acceptance. By including a transfer function for the transverse momentum of each incident particle (in addition to the transfer functions for the outgoing legs of the matrix element), we can successfully account not only for ISR that is visible in the detector, but also for the case when the ISR does not produce visible jets. We

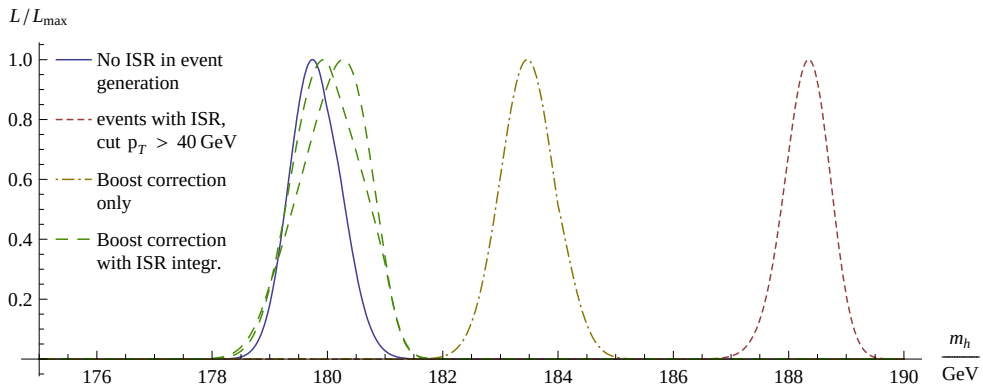

Figure 5: Reconstruction of the Higgs boson mass from a matrix element likelihood fit to 1000 hadron-level di-lepton events at the LHC with $\sqrt{s} = 14$ TeV. A Higgs mass of $m_h = 180$ GeV has been used for the event generation. The different curve correspond to the following setups: idealized situation without ISR in the event generation (solid curve); ISR included in the simulation but no correction (short dashed); purely kinematical boost correction (dash-dotted); boost correction with ISR transfer functions (long dashed). The two long-dashed curves correspond to ISR transfer functions tuned to $t\bar{t}$ and $h \to WW$ Monte-Carlo events, respectively. The likelihood reflects statistical errors only.

use a two-component transfer function, employing a double-Gaussian if the measured ISR $p_{\mathrm{T}}^{\mathrm{vis}}$ is non-zero, and a single Gaussian in log-space for zero $p_{\mathrm{T}}^{\mathrm{vis}}$:

$$W_{\mathrm{ISR}}(p_{\mathrm{T}}, p_{\mathrm{T}}^{\mathrm{vis}}) = \begin{cases} \frac{1}{\sqrt{2\pi}(a_2+a_3 a_5)} \left[e^{-(p_{\mathrm{T}}-p_{\mathrm{T}}^{\mathrm{vis}}-a_1)^2/(2a_2^2)} + a_3\, e^{-(p_{\mathrm{T}}-p_{\mathrm{T}}^{\mathrm{vis}}-a_4)^2/(2a_5^2)} \right], & \text{for } p_{\mathrm{T}}^{\mathrm{vis}} > p_{\mathrm{T}}^0, \\ \frac{1}{\sqrt{\pi}\, b_2\, p_{\mathrm{T}}}\, e^{-(\log(p_{\mathrm{T}})-b_1)^2/(2b_2^2)} & \text{for } p_{\mathrm{T}}^{\mathrm{vis}} < p_{\mathrm{T}}^0, \end{cases}$$

$$\text{with } a_i = b_{i0} + b_{i1}\sqrt{p_{\mathrm{T}}} + b_{i2} p_{\mathrm{T}}. \tag{14}$$

The boundary p_{T}^0 between the two regions should be chosen near the sensitivity limit of the detector (typically a few GeV), but we have checked that the results are not appreciably affected by varying p_{T}^0 between 5 and 15 GeV.

The free parameters b_i, b_{ij} in (14) are tuned to Monte Carlo simulated data, and it has been checked that the transfer function provides a good approximation to the Monte Carlo data both for small (a few GeV) and large ($\sim$ 100 GeV) values of p_{T}. This tune effectively accounts for Sudakov factors, as well as detector acceptance effects. When using ISR transfer functions one needs to integrate over the partonic p_{T} of each leg, so that the total integration dimension is increased by two. Nevertheless, when using an adaptive algorithm like Vegas [13], the integration time grows only by a factor of less than 10.

The increase in the number of degrees of freedom also leads to an increase of the width of the curve—however, the expected reduction in systematic effects and stability of the likelihood result due to the better control of QCD radiation using this method should by far make up for this.

Fig. 5 demonstrates the effect of the boost correction without and with ISR transfer functions for the Higgs production process (6). The plot shows that the ISR transfer functions

properly take into account the typical energy resolution and jet smearing effects and the fit result is consistent with the input value $m_h = 180$ GeV.

Note that Fig. 5 shows two curves for the result with ISR transfer functions, which correspond to transfer functions tuned to $t\bar{t}$ and $h \to WW$ Monte-Carlo events, respectively. The likelihood curves are almost identical for the two cases, which demonstrates that the transfer functions are quite insensitive to the hard process.

For the case of top-quark pair production, the fit result for the boost correction with ISR transfer functions is shown by the long-dashed curve in Fig. 4. It agrees very well with the input value $m_t = 175$ GeV, but in contrast to Higgs production, the purely kinematical boost correction is already satisfactory so that the inclusion of the transfer functions does not significantly improve the results.

Since the integration over ISR transfer functions helps to improve the MEM likelihood fit, one could wonder whether it might be sufficient to ignore the measured ISR momenta altogether and instead simply integrate over the p_{T} of ISR, weighted by the second line of eq. (14). We have tested this idea, but found that the results of such a fit are inconsistent with the true input values of m_t or m_h, respectively. Similar to the corresponding case without integration over p_{T} (dashed curves in Figs. 4 and 5), the best-fit values come out too large. This indicates that it is still important to include information about the observed QCD radiation jets into the fit, even if this information is distorted by detector effects.

So far we have shown that the boost correction method with ISR transfer functions is a robust and practical technique for dealing with initial-state QCD radiation in experimental likelihood fits based on the MEM. It remains to check how our method is affected by systematic uncertainties. The largest systematic uncertainty is expected to be related to the jet energy scale. This uncertainty can be taken into account by keeping the jet energy scale as a free parameter in the fit [3]. However, an extensive determination of the statistical and systematic uncertainties relating to the different methods (which are expected to be larger than the purely statistical uncertainties given by the likelihood fits in the figures), using pseudo-experiments with varying input masses and simulation parameters, is beyond the scope of this paper.

We will here instead focus on theoretical systematic error sources. As already mentioned above, we have checked that the variation of the lower p_{T} cutoff for ISR jets within reasonable ranges has a negligible effect on the fit results. Similarly, is has been shown that the ISR transfer functions are approximately universal and depend very little on the details of the hard scattering process (see Fig 5).

Furthermore, we estimate the systematic error stemming from the parton distribution functions (PDFs) by comparing fit results for CTEQ6L1 and CTEQ6M PDFs [12]. Here we only modify the PDFs in the MEM fit, while in both cases using the same event file and transfer functions, which have been determined with CTEQ6L1 PDFs. We find a negligible difference between the results for CTEQ6L1 and CTEQ6M PDFs and thus conclude that the systematic error from this source is very small.

Finally, missing virtual loop corrections in the hard matrix element are expected to have a very small influence on the detailed kinematics of the events. Since the matrix element

method is not making use of the total cross section for the determination of quantities such a masses and spins, such corrections are expected to have a negligible impact. We have explicitly checked this by running the same analyses on events generated using POWHEG [14], with no significant difference in the results. The reader should note, however, that in order to ensure a well-defined meaning of quantities such as masses at sub-GeV precision, this procedure should, in the long run, be developed to work at full NLO level.

5 Conclusions

The Matrix Element Method (MEM) is a powerful tool for analyzing processes with invisible particles in the final state at hadron colliders. For each experimental event, the MEM computes a likelihood that this event agrees with a given theoretical process supplied in the form of the corresponding squared matrix element. However, the MEM uses matrix elements with a fixed number of external partons, making it difficult to include the high-multiplicity initial state radiation (ISR) expected to be abundant at the LHC. In this paper, it has been shown explicitly that initial-state QCD radiation cannot be ignored in MEM fits, without risk of unstable and biased results. The simplest way to circumvent this problem, by applying a veto on events with sizeable ISR, is not acceptable since this cut would need to be so severe that the statistics of the signal event sample would be significantly depleted.

We have proposed a method to include the effect of ISR by correcting the momenta of the incident partons in the matrix element on an event-by-event basis. Concretely, the incoming parton momenta are boosted by the transverse momenta of the ISR. The effectiveness of the method has been demonstrated by carrying out a MEM fit for two characteristic physics processes with invisible particles in the final state, $pp \to t\bar{t} \to b\bar{b}l^+l^-\nu\bar{\nu}$ and $pp \to h \to W^+W^- \to l^+l^-\nu\bar{\nu}$.

As a first step, simulated parton-level events were used to show that this boost correction significantly improves the result of the likelihood fit, such that the fitted masses of the top quark or Higgs boson are fully consistent with the respective input values. As a second step, we applied the boost correction method to a more realistic situation with fully hadronized events that were sent through a fast detector simulation. In this case, detector effects will typically lead to a mismatch between the reconstructed and the true transverse momenta of the ISR. This difference can be taken into account by including transfer functions for the incident particles into the likelihood fit. The transfer functions parametrize the distribution of reconstructed transverse momenta for a given partonic transverse momentum, as obtained from Monte Carlo data. As a byproduct, the transfer functions also effectively capture the effect of showering, Sudakov factors, and hadronization. We found that the boost correction method with transfer functions yields stable MEM fit results in excellent agreement with the underlying input values.

The proposed method increases the computing time for the likelihood fit only by a moderate amount (less than a factor of ten in all situations that we have studied). Furthermore it is very robust under the influence of theoretical systematic uncertainties.

In conclusion, our results demonstrate that the boost correction method with ISR transfer

functions is a simple and effective technique for treating ISR in MEM likelihood fits. It is however important to validate our findings in a realistic experimental simulation with a proper treatment of experimental systematic effects.

Acknowledgements

The authors are grateful to D. Whiteson, K. Cranmer and T. Plehn for interesting discussions and insights. O. M. would also like to thank F. Maltoni for his constant support. This project was supported in part by the National Science Foundation under grant no. PHY-0854782, the HEPTOOLS EU network through Marie Curie program RTN MRTN-CT-2006-035505, by Belgian Technical and Cultural Affairs through the Interuniversity Attraction Pole P6/11, and by Computational Resources on PittGrid (`www.pittgrid.pitt.edu`). The work of J. A. was supported by NCTS under grant number NSC 98–2119–M–002–001. J. A. and A. F. are thankful to the Aspen Center for Physics, where this project was initiated.

References

[1] For a recent review of mass measurement methods see A. J. Barr and C. G. Lester, J. Phys. G **37**, 123001 (2010), and references therein.

[2] K. Kondo, J. Phys. Soc. Jap. **57**, 4126 (1988);
K. Kondo, J. Phys. Soc. Jap. **60**, 836 (1991);
R. H. Dalitz and G. R. Goldstein, Phys. Rev. D **45**, 1531 (1992);
J. Estrada, FERMILAB-THESIS-2001-07 (2001);
F. Canelli, FERMILAB-THESIS-2003-22 (2003).

[3] B. Abbott *et al.* [D0 Collaboration], Phys. Rev. D **60**, 052001 (1999);
V. M. Abazov *et al.* [D0 Collaboration], Nature **429**, 638 (2004);
A. Abulencia *et al.* [CDF Collaboration], Phys. Rev. D **74**, 032009 (2006);
V. M. Abazov *et al.* [D0 Collaboration], Phys. Rev. D **78**, 012005 (2008);
T. Aaltonen *et al.* [CDF Collaboration], Phys. Rev. Lett. **101**, 252001 (2008);
T. Aaltonen *et al.* [CDF Collaboration], CDF/PHYS/TOP/PUBLIC/10191 (2010).

[4] J. Alwall, A. Freitas and O. Mattelaer, in *Proceedings of SUSY09: 17th International Conference on Supersymmetry and the Unification of Fundamental Interactions*, eds. G. Alverson, P. Nath and B. Nelson, AIP Conf. Proc. **1200**, 442 (2010) [arXiv:0910.2522].

[5] T. Sjöstrand, S. Mrenna and P. Z. Skands, JHEP **0605**, 026 (2006).

[6] A. Abulencia *et al.* [CDF Collaboration], Phys. Rev. D **75**, 031105 (2007);
F. Fiedler, A. Grohsjean, P. Haefner and P. Schieferdecker, Nucl. Instrum. Meth. A **624**, 203 (2010).

[7] T. Plehn, D. Rainwater and P. Z. Skands, Phys. Lett. B **645**, 217 (2007);
J. Alwall, S. de Visscher and F. Maltoni, JHEP **0902**, 017 (2009).

[8] J. Conway, PGS 4, `http://www.physics.ucdavis.edu/~conway/research/software/pgs/pgs4-general.htm`.

[9] E. Boos *et al.* [CompHEP Collaboration], Nucl. Instrum. Meth. A **534**, 250 (2004).

[10] P. Artoisenet, V. Lemaître, F. Maltoni and O. Mattelaer, JHEP **1012**, 068 (2010).

[11] J. Alwall *et al.*, JHEP **0709**, 028 (2007).

[12] J. Pumplin, D. R. Stump, J. Huston, H. L. Lai, P. Nadolsky and W. K. Tung, JHEP **0207**, 012 (2002).

[13] G. P. Lepage, *"Vegas: An Adaptive Multidimensional Integration Program,"*, report CLNS-80/447 (1980).

[14] S. Frixione, P. Nason and G. Ridolfi, JHEP **0709**, 126 (2007);
P. Nason, JHEP **0411**, 040 (2004);
S. Frixione, P. Nason and C. Oleari, JHEP **0711**, 070 (2007);
S. Alioli, P. Nason, C. Oleari and E. Re, JHEP **1006**, 043 (2010).